Chitosan primes plant defence mechanisms against *Botrytis cinerea*, including expression of Avr9/Cf-9 rapidly-elicited genes

Daniel De Vega[1], Nicola Holden[1], Pete E Hedley[1], Jenny Morris[1], Estrella Luna[2*] and Adrian Newton[1*]

[1]The James Hutton Institute, Invergowrie, Dundee DD2 5DA, UK

[2]School of Bioscience, University of Birmingham, Edgbaston B15 2TT, UK

*Authors for correspondence: e.lunadiez@bham.ac.uk (+44 (0)1214148699) and adrian.newton@hutton.ac.uk (+44 (0)344 928 5428)

Funding Information: AHDB (HDC) Studentship CP105, BBSRC Future Leader Fellowship BB/P00556X/1 and BB/P00556X/2

Abstract

Current crop protection strategies against the fungal pathogen *Botrytis cinerea* rely on a combination of conventional fungicides and host genetic resistance. However, due to pathogen evolution and legislation in the use of fungicides, these strategies are not sufficient to protect plants against this pathogen. Defence elicitors can stimulate plant defence mechanisms through a phenomenon known as priming. Priming results in a faster and/or stronger expression of resistance upon pathogen recognition by the host. This work aims to study priming of a commercial formulation of the elicitor chitosan. Treatments with chitosan result in induced resistance in solanaceous and brassicaceous plants. In tomato plants, enhanced resistance has been linked with priming of callose deposition and accumulation of the plant hormone jasmonic acid (JA). Large-scale transcriptomic analysis revealed that chitosan primes gene expression at early time-points after infection. In addition, two novel tomato genes with a characteristic priming profile were identified, Avr9/Cf-9 rapidly-elicited protein 75 (*ACRE75)* and 180 *(ACRE180)*. Transient and stable overexpression of *ACRE75*, *ACRE180* and their *Nicotiana benthamiana* homologs, revealed that they are positive regulators of plant resistance against *B. cinerea*. This provides valuable information in the search for strategies to protect Solanaceae plants against *B. cinerea*.

Keywords

Chitosan, *Botrytis cinerea* (Grey mould), Callose, Induced Resistance, Priming, *Solanum lycopersicum* (tomato), Solanaceae, Transcriptomics

Introduction

Crop yield losses of 20-40% of total agriculture productivity can be attributed to pests and diseases (Oerke, 2006, Savary et al., 2012). Of these threats, the pathogen *Botrytis cinerea* causes annual losses of $10-$100 billion, as it reduces crop yield before harvest or leads to waste and spoilage post-harvest. It is the causative agent of grey mould disease in tomato and many other economically important crops, such as pepper, aubergine, grape, lettuce and raspberry. *B. cinerea* is a fungal generalist (broad-host range) and considered to be a model necrotrophic pathogen (Williamson et al., 2007). Effective control include the use of conventional crop protectants (e.g. fungicides) and resistant varieties as well as sanitation and environmental control. However, rapid pathogen evolution can result in the loss of efficacy of resistance sources and fungicides (Pappas, 1997, Williamson et al., 2007). In addition, the use of pesticides is strictly limited by European regulations due to human health and environment risk and hazard assessment changes. New alternative strategies are therefore needed. Exploiting the plant's defence system to provide protection against these threats has emerged as a potential strategy against pathogen infection and disease (Luna, 2016).

Plant endogenous defences is activated by elicitor molecules resulting in induced resistance (IR) (Mauch-Mani et al., 2017), since they are able to mimic pathogen-inducible defence mechanisms (Aranega-Bou et al., 2014). Induced resistance works via two different mechanisms: direct activation of systemic plant defences after signal recognition and; priming, a mechanism that initiates a wide reprogramming of plant processes, considered to be an adaptive component of induced resistance (Mauch-Mani et al., 2017). Priming has been demonstrated to be the most cost-effective mechanism of induced resistance in terms of plant development as there is no direct relocation of plant resources from growth to defence until it

is necessary (van Hulten et al., 2006). Studies have already shown that low elicitor doses can enhance resistance to pests without interfering with crop production (Redman et al., 2001). Elicitor-induced priming has been demonstrated to last from a few days (Conrath et al., 2006) to weeks (Worrall et al., 2012) after treatment and even through subsequent generations (Ramírez-Carrasco et al., 2017, Slaughter et al., 2012).

Priming can have multiple effects on plant defences, which vary depending on the type of plant-pathogen interaction. Defence priming enables the plant to fine-tune immunity responses through enhancement of the initial defences. These is achieved through different mechanisms that act at specific defence layers (Mauch-Mani et al., 2017). For instance, cell-wall fortification and effective production of reactive oxygen species (ROS) has been used as a marker for the expression of priming responses. Hexanoic acid (Hx) primes cell-wall defences through callose deposition and redox processes in tomato cultivars against *B.cinerea* (Aranega-Bou et al., 2014). In *Arabidopsis thaliana*, BABA and benzothiadiazole (BTH)-induced priming is also based on an increase in callose deposition (Kohler et al., 2002, Ton et al., 2005). Priming also results in transcriptomic changes. Gene expression analysis of *A. thaliana* after BABA treatment was used to identify a transient accumulation of SA-dependent transcripts, including that of *NPR1*, which provides resistance against *Pseudomonas syringae* (Zimmerli et al., 2000). Changes in metabolite accumulation have been shown to mark priming of defence also. For instance, defence hormone profiling has shown that accumulation of JA and JA-derivatives mediates priming of mycorrhizal fungi (Pozo et al., 2015). Moreover, untargeted metabolomic analysis have identified different compounds, including kaempferol (Król et al., 2015), quercetin, and indole 3 carboxylic acid (I3CA) (Gamir et al., 2014), that drive priming responses.

Several elicitors have been described to induce resistance mechanisms in tomato against *B. cinerea*. For instance, BABA has been demonstrated to provide long-lasting induced resistance against *B. cinerea* in leaves (Luna et al., 2016) and in fruit (Wilkinson et al., 2018). In addition, the plant defence hormone JA has also been linked to short-term and long-term induced resistance in tomato against *B. cinerea* (Luna et al., 2016, Worrall et al., 2012). To date, however, few studies have investigated elicitor-induced priming in tomato against *B. cinerea*. One of them showed that Hx-induced priming is based on callose deposition, the expression of tomato antimicrobial genes (e.g. protease inhibitor and endochitinase genes), and the fine-tuning of redox processes (Aranega-Bou et al., 2014, Finiti et al., 2014). Therefore, evidence is building in tomato, that induced resistance against *B. cinerea* can be based on priming also.

In this study we investigated whether the chitin de-acetylated derivative, chitosan, triggers priming of defence in tomato against *B. cinerea*. Chitosan as a plant protection product is considered 'generally recognised as safe' (Raafat and Sahl, 2009) that is effective in protecting strawberry, tomato and grape against *B. cinerea* (Muñoz and Moret, 2010, Romanazzi et al., 2013). Different studies have shown that its effect on crop protection results from induction of defence mechanisms (Sathiyabama et al., 2014) and direct antimicrobial activity (Goy et al., 2009). However, treatments with chitosan require infiltration into the leaves to trigger a robust effect (Scalschi et al., 2015) making it an unsuitable method of application in large-scale experiments or studies that take into consideration first barrier defence strategies. Here, we have addressed whether treatment with a water-soluble formulation of chitosan results in induced resistance phenotypes and in priming of cell wall defence and defence hormone accumulation. In addition, whole-scale transcriptome analysis was performed to identify candidate genes that are driving expression

of priming. Our findings, together with the outlined characteristics of chitosan, make this substance a suitable candidate for extensive application as a component of Integrated Pests (and disease) Management (IPM) for the protection of crops against fungal pathogens.

Material and Methods

Plant material and growth conditions

Tomato cv. Money-maker seeds were used in the described experiments. Unless otherwise specified, seeds were placed into propagator trays containing Bulrush peat (Bulrush pesticide-free black peat, low nutrient and low fertilizer mix) and a top layer of vermiculite and left at 20 °C until germination. Germinated seeds were transplanted to individual pots containing Bulrush soil (pesticide-free compost mix and nutrient and fertilizer rich) in a growth cabinet for 16h - 8h / day-night and 23°C / 20°C cycle C at ~150 μE m^{-2} s^{-1} at ~ 60% relative humidity (RH). *Nicotiana benthamiana* seeds were cultivated in a similar manner specified for tomato for 16h - 8h/ day-night cycle; 26°C / 22°C at ~150 μE m^{-2} s^{-1} at ~ 60% relative humidity (RH). Aubergine (*Solanum melongena*) cv. Black Beauty seeds were placed into propagators containing Bulrush peat and a layer of vermiculite on the top and incubated at 20°C for 1-2 weeks until germination. Seedlings were then transplanted to individual pots containing Bulrush soil and grown and cultivated as for tomato. *Arabidopsis thaliana* (hereafter referred to as Arabidopsis) Columbia-0 (Col-0) and transgenic lines were grown in a soil mixture of 2/3 Levington M3 soil and 1/3 sand for 8h - 16h/day - night and 21ºC / 18ºC cycle at ~150 μE m^{-2} s^{-1} at ~ 60% RH. Ten-day-old plants were transplanted to individual pots.

Chemical treatment

All experiments were performed using a commercial, water-soluble chitosan formulation, known as ChitoPlant (ChiPro GmbH, Bremen, Germany) (Romanazzi et al., 2013, Younes et al., 2014). ChitoPlant, referred to as chitosan latterly, was freshly prepared in water to the specific concentrations (please see figure legends for details). Treatments were performed by foliar spraying of chitosan solution (with 0.01% Tween20) directly onto leaves.

Botrytis cinerea cultivation, infection and scoring

B. cinerea R16 (Faretra and Pollastro, 1991) was used in all experiments and was kindly provided by Dr Mike Roberts (Lancaster University). Cultivation of the fungus and infection of tomato-based experiments were performed as described (Luna et al., 2016). For *N. benthamiana*, 2-3 detached leaves were inoculated with 6µl inoculum solution containing 2 x 10^4 spores/ml of *B. cinerea*. Infected leaves were kept at 100% RH by sealing the trays and placed in the dark before disease assessment. Arabidopsis infections were performed as previously described (La Camera et al., 2011) with a few modifications. Leaves were inoculated with 5µl inoculum solution containing ½ strength of potato dextrose broth (PDB – Difco at 12 g/l) and 5 x 10^5 spores/ml. Infected Arabidopsis plants were put in a sealed tray at 100% RH and moved back to the growth cabinet. Infections of *S. melongena* plants were performed by drop inoculating detached leaves with a spore solution of *B. cinerea* containing 2 x 10^4 spores/ ml. For all pathosystems, disease was scored by measuring lesion diameters with an electronic calliper (0.1 mm resolution) on different days post infection.

Plant growth analysis

Relative growth rate (RGR) was used to analyse tomato growth after chitosan treatment as described (Luna et al., 2016). Growth analysis of Arabidopsis plants was performed by measuring rosette perimeter using Photoshop CS5 (Vasseur et al., 2018).

175

176

177 **Callose deposition assays**

178 For analysis of callose deposition after chitosan treatment, material from tomato and
179 Arabidopsis plants with different concentrations of chitosan were collected 1 day after
180 treatment (dat) and placed in 96% (v/v) ethanol in order to destain leaves. Aniline blue was
181 used to stain callose deposits as described previously (Luna et al., 2011). Analysis of callose
182 associated with the infection by *B. cinerea* in tomato leaves was performed as described
183 (Rejeb et al., 2018) with some modifications. Briefly, infected tomato leaf samples were
184 collected and placed in 96% (v/v) ethanol 1 day after infection with *B. cinerea* and allowed to
185 destain. Destained material was hydrated with 0.07 M phosphate buffer (pH 9.0) for 30 min
186 and then incubated for 15 min in 0.1% (w/v) aniline blue (Sigma-Aldrich) and 0.005% (w/v)
187 fluorescent brightener (Sigma-Aldrich). Solutions were then replaced with 0.1% (w/v) aniline
188 blue and incubated for 24h in the dark prior to microscopic analysis. All observations were
189 performed using an UV-epifluorescence microscope (GXM-l2800 with GXCAM HiChrome-
190 MET camera). Callose was quantified from digital photographs by the number of yellow
191 pixels (callose intensity). Infection-associated callose was scored and analysed in a similar
192 way but callose intensity was expressed relative to fungal lesion diameters. Image analyses
193 were performed with Photoshop CS5 and ImageJ.

194 **Chitosan antifungal activity *in vitro* assay**

195 *B. cinerea* mycelial growth assessment was performed using Potato Dextrose Agar (PDA) as
196 culture media with different concentrations of chitosan (1%, 0.1%, 0.01% w/v). PDA was
197 autoclaved and then chitosan and the fungicide Switch (as positive fungicide control) (1%,
198 0.1%, 0.01% w/v) were added directly to PDA as it cooled. One 5 mm diameter agar plugs of
199 actively growing *B. cinerea* mycelium was added per plate. Five plates per treatment were

sealed with parafilm and then incubated under controlled conditions (darkness and 24°C). After 4 days, the mean growth of the fungus was determined by measuring two perpendicular diameters and calculating the mean diameter.

High-Pressure Liquid Chromatography (HPLC) - Mass Spectrometry (MS)

Healthy and infected tomato leaf tissues were harvested in liquid nitrogen and subsequently freeze-dried for 3 days. Freeze-dried samples were ground in 15 mL Falcon tubes containing a tungsten ball in a bead beater. Ten mg of each sample was used for hormone extraction. Sample extraction, HPLC-MS quantitative analysis of plant hormones and data analysis were performed as described (Forcat et al., 2008). Accurate quantification of ABA, SA and JA used the deuterated internal standards added during sample extraction (Forcat et al., 2008) and concentrations were calculated using standard concentration curves. Relative accumulation of jasmonic acid-isoleucine (JA-Ile) were obtained by calculations of % peak areas among samples.

Transcriptome analysis

Four conditions were analysed using microarrays: **(i)** ddH_2O-treated and non-infected plants (Water + Mock); **(ii)** Chitosan-treated and non-infected plants (Chitosan + Mock); **(iii)** ddH_2O-treated and *B. cinerea*-infected plants (Water + *B. cinerea*); **(iv)** Chitosan-treated and *B. cinerea*-infected plants (Chitosan + *B. cinerea*). Inoculations were performed four days after treatment (dat) with chitosan, and leaf discs from four independent plants (biological replicates) per treatment were sampled at 6, 9 and 12 h post-inoculation (hpi) with mock or *B. cinerea* spores. Total RNA was extracted with an RNeasy Plant Mini Kit (Qiagen) as recommended. A custom 60-mer oligonucleotide microarray was designed using eArray (https://earray.chem.agilent.com/earray/; A-MTAB-667 and E-MTAB-8868; www.ebi.ac.uk/arrayexpress/) from predicted transcripts (34,616 in total) of the *S.*

lycopersicum (ITAG 2.3) genome. Experimental design is detailed at E-MTAB-8868; www.ebi.ac.uk/arrayexpress/. Two-channel microarray processing was utilised, according to the Low Input Quick Amp Labelling Protocol v. 6.5 (Agilent). Microarray images were imported into Feature Extraction software (v. 10.7.3.1; Agilent) and data extracted using default parameters. Data were subsequently imported into Genespring software (v. 7.3; Agilent) for subsequent pre-processing and statistical analysis. Following Lowess normalisation, data were re-imported as single-colour data. Data were filtered to remove probes that did not have detectable signal in at least 3 replicates, leaving 22,381 probes for statistical analysis.

Analysis of Variance (2-way ANOVA; p-value ≤0.01, Benjamini-Hochberg false discovery rate correction) was used to identify differentially expressed genes (DEGs) for the factors 'Treatment' (3,713 DEGs), 'Time' (6,920), and 'Treatment-Time interaction' (186). Subsequently, pairwise Student's T-tests were performed (Volcano plots: P-value ≤0.05, 2-fold cut-off) on the global set of 8,471 DEGs for each of the three test treatments (Chitosan + Mock, Water + Mock and Chitosan + *B. cinerea*) compared to control (Water + Mock) at each time point. Venn diagrams were used at each time point to identify common and specific DEGs.

Panther gene ontology (GO) term enrichment analysis

Panther software (Thomas et al., 2003) was used to visualise DEG products in the context of biological pathways and/or molecular functions, using default settings. Functional enrichment analysis was performed using DEG lists for Chitosan + *B. cinerea* and Water + *B. cinerea* treatments at 6 hpi. 'Biological processes' and 'molecular functions' were selected using

248 PANTHER Overrepresentation Test (release 20170413) against *S. lycopersicum* (all genes in
249 database) and Bonferroni correction for multiple testing.
250

251 **DEG transcript co-expression analysis**

252 Two-way ANOVA was performed on the filtered microarray dataset at increased stringency
253 (p-value ≤0.01, Bonferroni false discovery rate correction) to identify 1,722 highly-
254 significant DEGs. Pearson's correlation was used with default settings in Genespring (v 7.3)
255 to generate a heatmap to help identify co-expressed transcripts (Figure 3b).
256

257 **Gene expression analysis**

258 Validation of *S. lycopersicum* transcriptomic analysis was performed by qRT-PCR of nine
259 candidate differentially expressed genes (DEGs), comparing gene expression values with
260 microarray. RNA samples were DNAse-treated with TurboDnase (ThermoFisher) and
261 complementary DNA (cDNA) was synthesized from 2.5 µg total RNA using Superscript III
262 reverse transcriptase (Invitrogen) as recommended with random hexamer/oligo dT primers.
263 RT-qPCR reactions were performed with specific *S. lycopersicum* oligonucleotide primers
264 (Table S4) purchased from Sigma-Aldrich. Gene primers and probes were designed using
265 Universal Probe Library (UPL) assay design centre (Roche Diagnostics Ltd.). RT-qPCR was
266 performed using FastStart Universal Probe Master Mix (Roche) and expression was
267 calculated against two reference genes (*SlActin-like* and *SlUbiquitin*) using the Pfaffl method
268 (Pfaffl, 2001).
269

270 **Gene cloning**

Orthologues of *SlACRE75* and *SlACRE180* were obtained from CDS and protein sequences BLAST analysis against Arabidopsis genome (TAIR10) for Arabidopsis sequences, or a reciprocal best BLAST hits (RBH) (Ward and Moreno-Hagelsieb, 2014) test was performed (Sol Genomics Network) for *N. benthamiana*, termed *NbACRE75* and *NbACRE180*, respectively. Best CDS and protein hits were identified, being Niben101Scf03108g12002.1 and Niben101Scf12017g01005.1 for SlACRE75 and SlACRE180 respectively; termed NbACRE75 and NbACRE180 onwards. Flanking the (i) *SlACRE75*, (ii) *SlACRE180*, (iii) *NbACRE180* and (iv) *NbACRE75* coding sequences (CDS), Gateway® cloning was used to design and produce overexpression constructs for the gene candidates for a N-terminal GFP:ACRE fusion protein per insert (Reece-Hoyes and Walhout, 2018). Briefly, pUC57 plasmids containing *SlACRE75*, *SlACRE180*, *NbACRE75* and *NbACRE180* coding sequences were chemically synthesized by GenScript. For *SlACRE75*, *SlACRE180*, *NbACRE75* and *NbACRE180*, cDNAs from pUC57 entry vector were transformed by electroporation into *Escherichia coli* strain DH10B and transferred by a recombinant LR reaction of Gateway cloning (Clonase II enzyme mix Kit, Thermo Fisher) into pB7WGF2 (Karimi et al., 2002).

Transient expression in *Nicotiana benthamiana*

Agrobacterium tumefaciens, strain GV3103, carrying plasmids with expression constructs (i) pB7WGF2:35S:GFP:SlACRE75; (ii) pB7WGF2:35S:GFP:SlACRE180; (iii) pB7WGF2:35S:GFP:NbACRE180; (iv) pB7WGF2:35S:GFP:NbACRE75 and; (v) pB7WGF2:35S:GFP (empty vector), were grown in YEP medium (containing 50 µg/ ml rifampicin, 100 µg/ ml spectinomycin, and 25 µg/ ml gentamicin) for 24 h with continuous shaking at 28°C. Overnight cultures were collected by centrifugation, resuspended in Agromix/infiltration buffer (10 mM $MgCl_2$: 10 mM MES) and 200 µM acetosyringone (pH 5.7) and diluted to a final volume of 20 ml at OD_{600} of 0.1. Cultures were infiltrated into

296 leaves of 4-week-old *N. benthamiana* plants using 1 ml needleless syringes. One day after
297 agroinfiltration, 1-2 leaves per plant were excised for *B. cinerea* infection assays (as
298 described above). These experiments were repeated once.
299
300
301 **Confocal microscopy analysis**
302 For the analysis of the subcellular localization, *A. tumefaciens* GV3101 carrying plasmids
303 with expression constructs were co-infiltrated with pFlub vector (RFP-peroxisome tagged
304 marker) into leaves of 4-week-old *N. benthamiana* CB157 (nucleus mRFP marker) and
305 CB172 (ER mRFP marker) reporter lines using 1 ml needleless syringes. Two days after
306 infiltration, leaves were excised and prepared for confocal microscopy. GFP and mRFP
307 fluorescence was examined under Nikon A1R confocal microscope with a water-dipping
308 objective, Nikon X 40/ 1.0W. GFP was excited at 488 nm from an argon laser and its
309 emissions were detected between 500 and 530 nm. mRFP was excited at 561 nm from a
310 diode laser, and its emissions were collected between 600 and 630 nm.

311 **Western blot analysis**
312 Leaves from *N. benthamiana* leaves infiltrated with *A. tumefaciens* GV3101 carrying
313 plasmids with expression constructs were excised, ground and proteins extracted as
314 previously described (Gilroy et al., 2011, Yang et al., 2016). Western blotting was performed
315 as previously described (Qin et al., 2018). Detection of GFP was performed using a
316 polyclonal rabbit anti-GFP antibody (1:4,000 dilution) and secondary anti-mouse antibody
317 (IG HRP 1:10,000) according to the manufacturer's instructions. ECL development kit
318 (Amersham) detection was used according to the manufacturer's instructions.

319 **Transformation of *Arabidopsis thaliana* stable overexpression transgenic lines**

Arabidopsis overexpression plants were transformed using *A. tumefaciens* GV3101 carrying plasmids with expression constructs using the flower dipping method (Clough and Bent, 1998). Selection of Arabidopsis transformants and homozygous lines selection were performed as described (Luna et al., 2014). Resistance was tested against *B. cinerea* as described before. Two independent homozygous overexpression lines were obtained per construct.

Pathosystem statistics

Statistical analysis of induced resistance and growth phenotypes were performed as described (Luna et al., 2016). Data analysis was performed using SPSS Statistics 23 and GenStat® 18th Edition (VSN International, Hemel Hempstead, UK). Statistical analysis of resistance phenotypes in Arabidopsis overexpression lines was done by ANOVA with 'construct' as a single treatment factor at 10 levels: Col-0 (wild-type treatment); two empty vector lines 'EV 3.1' and 'EV 4.1'; 'SlACRE75 1.1' and 'SlACRE75 2.1'; 'SlACRE180 1.2' and 'SlACRE180 3.1; 'NbACRE180 1.1' and 'NbACRE180 2.1'; and 'NbACRE75 1.1'. The replicate units were individual plants of which there were 8-16 for each construct. Measurements of four lesions were recorded for each plant. Random effects were modelled as plant + plant × lesion to capture the plant-to-plant and within-plant variation. As part of the ANOVA, specific planned (non-orthogonal) contrasts were included to test for significant differences between the mean for each construct line compared to Col-0.

Results

Identification and characterisation of a novel chitosan formulation in its ability to induce resistance against *Botrytis cinerea*

We tested the water-soluble chitosan-based commercial formulation ChitoPlant, from hereafter termed chitosan, in its capacity to induce resistance against the fungal pathogen *B. cinerea*. Treatments of chitosan demonstrated that this elicitor successfully triggers resistance in tomato (Figure 1a), Arabidopsis (Figure 1b) and aubergine (Fig S1) against *B. cinerea*. In tomato, chitosan significantly decreased necrotic lesion size in all concentrations compared with control plants (Fig 1a). The resistance phenotype induced by chitosan had a dose-dependent effect at the two high concentrations (1% and 0.1%), however, the lowest concentration (0.01%) induced a level of resistance in between 0.1% and 1% treatments. In Arabidopsis, chitosan treatment resulted in induced resistance in a concentration-dependent manner, with 1% having the strongest effect (Fig 1b). In aubergine, chitosan treatment resulted in differences in lesion diameter in all concentrations compared to water-treated control plants (Figure S1), however, post-hoc analysis demonstrated that 0.1% was the most effective concentration.

We then tested whether chitosan induces callose deposition in a similar manner to other chitosan formulations (Luna et al., 2011). Plants were treated with increasing concentrations of chitosan one day before aniline blue staining. In both plant species, treatments with chitosan resulted in a direct induction of callose. The lowest concentrations of 0.001% and 0.01% in tomato and Arabidopsis, respectively, triggered the strongest effect (Fig 1 c and d).

To determine any antifungal effect of chitosan, different concentrations were tested on *B. cinerea* hyphal growth *in vitro* and compared to different concentrations of the fungicide Switch (Syngenta). Whereas all concentrations of Switch arrested pathogen growth, only 0.1% concentration of chitosan or higher had an antifungal effect (Fig S2). However, the lowest concentration of chitosan tested (0.01 %) had no antifungal effect compared to the

369 control. This shows a concentration threshold for chitosan-direct antifungal activity against *B.*
370 *cinerea*. Since 0.01% chitosan had no antifungal effect, but reduced *B. cinerea* lesions and
371 induced callose formation, this concentration was selected for more in-depth analysis.
372
373 **Analysis of priming mechanisms marking chitosan-induced resistance**
374 We tested whether induced resistance triggered by chitosan is mediated by priming
375 mechanisms through the assessment of its capacity to induced long-lasting resistance in distal
376 parts of the plants. Treatments with 1% chitosan induced long-lasting resistance against *B.*
377 *cinerea* of up to 2 weeks after initial treatment of tomato plants (Fig 2a).
378
379 In order to assess whether treatments with chitosan directly affects plant development, we
380 tested plant growth one week after treatment with 1% chitosan. These experiments revealed
381 that chitosan treatment triggers a statistically significant growth promotion, therefore
382 indicating that induced resistance by chitosan does not negatively impact plant development
383 (Fig S3a).
384
385 To study whether chitosan induced resistance (IR) was based on known mechanisms of
386 priming, callose and hormone profiling analysis were performed after subsequent infection.
387 Treatment with chitosan resulted in the accumulation of approximately twice the callose
388 deposited at the site of attack compared to plants treated with water (Fig 2b,c). In addition,
389 mass spectrometry profiling of defence-dependent hormones demonstrated that chitosan-
390 induced resistance is mediated specifically by accumulation of jasmonic acid (JA) (Fig 2c)
391 and its amino acid conjugate JA- isoleucine (JA-Ile, Fig S3b). In contrast, no other impacts
392 were found in the concentration of other defence hormones such as salicylic acid (SA) and

393 abscisic acid (ABA) (Fig 2c). Thus, chitosan-IR is based on priming of callose at the
394 infection site and accumulation of JA and its conjugate JA-Ile.
395
396 **Transcriptional analysis of chitosan-induced resistance**
397 Priming of gene expression normally follows a characteristic pattern: differential expression
398 is low, transient or often non-detectable after treatment with the elicitor only (i.e. Chitosan +
399 Mock) and enhanced differential expression occurs upon subsequent infection (i.e. Chitosan
400 + *B. cinerea*) compared to infected plants that were not pretreated with the chemical (i.e.
401 Water + *B. cinerea*) (Conrath et al., 2006, Martinez-Medina et al., 2016). Importantly, the
402 expression kinetics are also key points for the establishment of priming. To further determine
403 the priming basis of chitosan-induced resistance, we performed whole transcriptomic analysis
404 at 6, 9 and 12 hours post infection (hpi) with *B. cinerea.* These time points were selected as
405 they cover the early, non-symptomatic start of the *B. cinerea* infection process. Unsupervised
406 data analysis was first performed to observe global changes in the experiment. For this, we
407 did a 2D principal component analysis (PCA) at different hours post infection. This analysis
408 shows that chitosan treatments did not trigger major changes in transcription, however, it was
409 the infection with *B. cinerea* which greatly impacts the experiment (Fig 3a). Moreover,
410 whereas separation can be observed between Mock- and *B. cinerea*-infected replicates at 9
411 and 12 hpi, no obvious differences could be seen at the early time point of 6 hpi.
412
413 Genes with similar expression profiles were grouped, resulting in the identification of 1,722
414 differentially-expressed genes (DEGs) across all three treatments and time points.
415 Hierarchical clustering separated the genes into four crude groups when compared to the
416 Water + Mock treatment at the first time point (6 hpi, Fig 3b): Cluster *i* consists of genes that
417 were repressed by *B. cinerea* infection; cluster *ii* represents genes induced by chitosan

418 treatment only; cluster *iii* includes genes repressed by *B. cinerea* infection and by treatment
419 of chitosan at the later time points; cluster *iv* consists of genes induced by *B. cinerea*
420 infection and by treatment of chitosan only (Fig 3b). Overall patterns aligned with the
421 previous finding that infection with *B. cinerea* had a large-scale, more extensive and
422 differential response on tomato transcription compared to treatment with chitosan (Fig 3a).
423 Moreover, the analysis demonstrates that application of chitosan results in a higher number of
424 genes repressed than induced, with the exception of some highly induced genes in cluster *iv*.
425 Distinct differences were evident between treatment with chitosan compared to infection with
426 *B. cinerea*, e.g. a large group of genes in cluster *iv* differentially induced by *B. cinerea* at 9
427 and 12 h, as well as a large group of genes repressed by the pathogen in cluster *i*. This
428 indicates that chitosan works as a priming agent that does not directly trigger major effects in
429 gene transcription.
430
431 To study the different signalling pathways and specific genes responsible for priming of
432 chitosan against *B. cinerea*, a two-way ANOVA identified 8,471 differentially expressed
433 genes (DEGs) among all three treatments and time points. This global list of DEGs was
434 subsequently used for focussed pairwise analysis to identify transcripts changing between
435 treatments at each time-point. Venn diagrams demonstrates that the effect of chitosan on its
436 own did not trigger major changes in gene transcription: only 15, 36 and 20 genes were
437 differentially expressed in Chitosan + Mock vs Water + Mock treatments at 6, 9 and 12 hpi,
438 respectively (Fig 3c). However, the effect of chitosan was much more pronounced after
439 plants had been infected with *B. cinerea*. This combination resulted in the differential
440 expression of 543, 2,011 and 2,967 genes at 6, 9 and 12 hpi, respectively, of which 260, 991
441 and 723 DEGs were induced only in the chitosan *B. cinerea* treatment (Fig 3c). In
442 comparison, Water + *B. cinerea* treatments displayed differential expression of 327, 1,134,

and 2,697 genes at 6, 9 and 12 hpi, respectively, of which 70, 116 and 501 DEGs were specific to the Water + *B. cinerea* treatment (Fig 3c). These results demonstrate that there is a subset of genes potentially responsible for chitosan-induced priming for a faster and more robust response against *B. cinerea.*

To further identify early-acting signalling pathways and genes involved in chitosan-induced priming, further analyses were performed on genes corresponding to the 260 probes differentially expressed only in the Chitosan + *B. cinerea* treatment at 6 hpi. Gene overrepresentation analysis was performed to identify biological processes and molecular functions of enriched genes. For biological processes, pathways such as response to stimulus, chemical and auxins were overrepresented (Table 1). Moreover, for molecular function, cysteine-type peptidase activity, transcription factor activity, sequence-specific DNA binding and nucleic acid binding transcription factor activity were enriched (Table 1).

Identification of genes primed by chitosan

To identify genes that could be involved in chitosan-induced resistance, gene expression profiles were scrutinized. First, qRT-PCR analysis of a subset of 9 genes was done to successfully validate the expression data of the microarray (Fig S4). Similar expression profiles were observed in the microarray and the qRT-PCR data, validating the data set. Priming profiles, i.e. subtle or non-detectable differential expression after chitosan treatment (i.e. Chitosan + Mock) and an increased differential expression after infection (i.e. Chitosan + *B. cinerea*) were identified. Transcripts of the earliest time point during the infection (6 hpi) were chosen to identify primed genes involved in early immune responses. Expression of the subset of 260 DEGs unique for Chitosan + *B. cinerea* treatment at 6 hpi (Fig 3c) were analysed over Water + Mock, Chitosan + Mock and water + *B. cinerea*. From the subset, 203

down-regulated (Table S1) and 57 genes were found to be up-regulated (Table S2). An over-representation test was performed to investigate gene ontology categories of the primed genes (Panther 14.0).

Among the 203 genes that were repressed during infection (Table S1), eleven transcripts were associated with cysteine-type peptidase activity. Other transcripts were grouped with photosynthesis, light harvesting in photosystem I activity. Moreover, several had a response to hormone activity; nine ethylene-responsive transcription factor and receptor genes were significantly down-regulated from -2,3 to -1,1 compared to Water + *B. cinerea*. Other notable genes with strong priming include those with proteolysis activity, with a range between -3 to -1,7 fold repressed. Other genes with repressed expression belong to auxin hormones and one to the ABA receptor (ABAPYL4). Furthermore, two genes of the little-known LATERAL ORGAN BOUNDARIES (LOB) were identified as repressed. Additional transcripts were functionally unassigned within the list.

Among the 57 differentially up-regulated genes (Table S2), there was one transcript encoding peroxidase activity with 2 fold increase compared to Water + *B. cinerea*, nine transcripts with protein kinase activity with between +1,1 to +2,1 fold, five transcripts with transcription regulatory activity, including SlMYB20, SLWRKY51 and SlWRKY72. Additional transcripts were functionally unassigned within the list.

Importantly, uncharacterised genes also show primed expression patterns. Of these, Avr9/Cf-9 rapidly elicited protein 75 (ACRE75; Solyc11g010250.1) was up-regulated 1,6-fold in Chitosan + *B. cinerea* in comparison to water + *B. cinerea* at 6 hpi (Table S2). ACRE genes have been previously studied and characterised as important genes involved in R gene-

493 mediated and ROS gene-independent early plant defence responses (Durrant et al., 2000) and
494 in response to methyl-jasmonate (MeJA) treatment (van den Burg et al., 2008). ACRE75
495 molecular functions are still to be deciphered and therefore research into its role and other
496 members of the ACRE gene family in priming of chitosan was pursued.
497
498 **Role of ACRE genes in induced resistance against *Botrytis cinerea***
499 In order to investigate whether other members of the ACRE gene family display a similar
500 priming profile to *ACRE75*, correlation analysis was performed on the subset of genes
501 differentially expressed at 6 hpi. Genes with statistically significant similar profiles were
502 identified (Table S3), which included *ACRE180* at a confidence value of 0.956. In addition,
503 analysis of the samples later in the experiment, confirmed that both *ACRE75* and *ACRE180*
504 are primed also at later time points (Fig S4).
505
506 In order to investigate whether primed expression of *ACRE75* and *ACRE180* genes may be
507 involved in enhanced disease resistance, genes from *S. lycopersium* and ortholog genes in *N.*
508 *benthamiana* were overexpressed using both transient and stable systems. For *SlACRE75*,
509 best match against *N. benthamiana* genome was Niben101Scf03108g12002.1 (termed
510 *NbACRE75*), sharing a 77.5% protein identity; (ii) For *SlACRE180*, the best match against the
511 *N. benthamiana* genome was Niben101Scf12017g01005.1 (termed NbACRE180), with
512 49.5% protein identity. Arabidopsis ortholog analysis failed to identify hits for *ACRE75* and
513 *ACRE1280* candidate genes. Constructs were produced with a fused GFP protein in the N-
514 terminus and protein integrity was confirmed via Western blot. Proteins extracted from *N.*
515 *benthamiana* leaves 48h after agro-infiltration and Western blot analysis confirmed that they
516 were the expected sizes (Fig S5). Subcellular location of proteins was analysed via confocal
517 microscopy of GFP fluorescence (Fig S6). Overexpression constructs were co-infiltrated with

RFP-marker pFlub vector (McLellan et al., 2013) (Fig S6a) into *N. benthamiana* reporter lines CB157 (nucleus mRFP marker - Fig S6b) and CB172 (ER mRFP marker - Fig S6c). Free GFP accumulated in both cytoplasm and nucleus (Fig S6d), whereas GFP-SlACRE75 and GFP-NbACRE75 fusions accumulated exclusively in the nucleus and nucleolus of *N. benthamiana* cells (Fig S6e,f). Furthermore, GFP-SlACRE180 fusion accumulated exclusively in ER (Fig S6g), whereas GFP-NbACRE180 fusion accumulation was exclusively in peroxisomes (Fig S6h).

To further investigate the impact of overexpression of *ACRE* genes in disease resistance, the 4 constructs containing GFP-SlACRE75, GFP-SlACRE180, GFP-NbACRE75 and GFP-NbACRE180, and GFP-empty vector (EV), were agro-infiltrated into leaves of *N. benthamiana* plants, which were subsequently challenged with *B. cinerea*. Chitosan-induced resistance against *B. cinerea* was proven effective in *N. bethamiana* (Fig 4a). All GFP-SlACRE75, GFP-SlACRE180, GFP-NbACRE75 and GFP-NbACRE180-infiltrated *N. benthamiana* leaves showed a significant decreased in *B. cinerea* necrotic lesion size compared with the EV control (Fig 4b). To further analyse *ACRE75* and *ACRE180* biological functions and to confirm their role in plant resistance against *B. cinerea*, Arabidopsis plants were transformed to constitutively overexpress GFP-SlACRE75, GFP-SlACRE180, GFP-NbACRE75 and GFP-NbACRE180 proteins. Homozygous lines were identified and growth phenotype of transgenic plants was analysed by measuring rosette perimeter. No statistically significant differences were identified (Fig S7). Five-week-old plants were infected with *B. cinerea* and disease was scored at 6 dpi. Transgenic GFP-SlACRE75, GFP-SlACRE180, GFP-NbACRE180 and GFP-NbACRE75 overexpression plants all showed an enhanced resistance phenotype and significantly decreased *B. cinerea* lesion sizes in comparison to Col-0 and GFP-EV controls (Fig 4c). Furthermore, GFP-SlACRE75 and its homolog GFP-

543 NbACRE75-overexpression plants showed a stronger resistance to *B. cinerea* than GFP-
544 SlACRE180 and GFP-NbACRE180 overexpression lines at 6 dpi (Fig 4c).
545

546 ## Discussion

547 We have assessed the capacity of chitosan to induce resistance against *B. cinerea* in different
548 plant species and have linked its effect with priming of defence mechanisms. We have
549 identified a formulation of chitosan that unlike some other formulations, can be easily
550 dissolved in water and does not require infiltration. This opens possibilities to identify early-
551 acting priming mechanisms in elicitor-induced resistance. Moreover, it enables opportunities
552 for upscaling the use of chitosan as an elicitor of resistance in large-scale experiments due to
553 the high-throughput nature of spraying the elicitor onto plants.
554 Treatments with chitosan resulted in induced resistance in *S. lycopersicum* (Fig 1a), *S.*
555 *melongena* (Fig S1), Arabidopsis (Fig 1b) and *N. benthamiana* (Fig 4a) at a range of
556 concentrations, which indicates that there are similar defence mechanisms acting in the
557 response to fungal PAMPs. Moreover, treatments with chitosan resulted in the activation of
558 basal resistance processes such as the deposition of callose at the cell wall (Fig 1c and d),
559 which is considered an important factor for penetration resistance against invading pathogens
560 (Oide et al., 2013). Expression of resistance was dependent on the concentration of chitosan
561 used in Arabidopsis. In contrast, in tomato and aubergine the levels of resistance did not
562 depend on the chitosan concentration. Moreover, chitosan-induced callose deposition in
563 tomato and Arabidopsis did not follow a classical dose-response curve and the most effective
564 treatments that activated callose were the lower concentrations of the elicitor (Fig 1c and d).
565 This is likely to be dependent on the antimicrobial effects of chitosan (Fig S2) at higher
566 concentrations. Other elicitors have been shown to trigger induced resistance phenomena at
567 lower concentrations. For example, meJA treatment results in more effective protection

against the pathogen *Fusarium oxysporum* f.sp. *lycopersici* when applied at lower concentrations (Król et al., 2015). In contrast, high doses of MeJA had detrimental effects on physiological processes and overall decreased protection efficiency. This, together with the observation that low concentrations of chitosan do not directly impact pathogen growth (Fig S2) suggests that there is a concentration threshold in the effect of chitosan-induced resistance.

Foliar applications of chitosan have been widely used to control disease development caused by numerous pests and pathogens (El Hadrami et al. 2010). However, few studies have investigated the role of chitosan as a priming agent and most have focused on its use as a seed priming elicitor mainly to improve germination and yield (Guan et al., 2009, Hameed et al., 2013). Here, we show that chitosan-induced resistance is based on priming of defence mechanisms. Our experiments confirmed that chitosan-induced resistance is not associated with growth reduction (Fig S3a), was durable and maintained for at least two weeks after treatment (Fig 2a), and that is based on a stronger accumulation of callose at the site of attackand accumulation of JA (Fig 2d) and JA-ile (Fig S3b). These results demonstrate that fungal growth arrest after chitosan treatment is not directly mediated by the toxicity effect of the chemical, as the infected leaves were formed after treatment and therefore were not sprayed with the elicitor. Moreover, these results demonstrate similar priming mechanisms after chitosan treatment to other elicitors, including Hx, which has been linked with priming of callose and JA against *B. cinerea* (Fernández-Crespo et al., 2017, Wang et al., 2014). Interestingly, however, despite many reported antagonistic and other crosstalk interactions between plant hormones (Robert-Seilaniantz et al., 2011), the concentrations of other plant hormones, SA and ABA, were not affected. This suggests that priming by chitosan does not

592 result in the downregulation of other hormone-dependent signalling pathways, thereby
593 maintaining an effective resistance status against other stresses.
594
595 In order to further explore priming of defence and to unravel the transcriptional mechanisms
596 behind chitosan-induced resistance, we performed transcriptome analysis. In our experiment,
597 using a concentration of chitosan that is associated with priming but with no direct
598 antimicrobial effect, we identified early-acting differential transcriptomic changes. Results
599 demonstrate that chitosan treatments do not result in major transcriptional changes (Fig 3a).
600 In contrast, comparison of treatment against Water + Mock revealed and Chitosan + *B.*
601 *cinerea* shows a higher number of DEGs (Fig 3b and c), thus responding to the priming
602 nature of the elicitor in the first instance.
603 Panther enrichment analysis showed that at 6hpi, the number of down-regulated DEGS was
604 more than three times up-regulated ones for Chitosan + *B. cinerea* (203 down-regulated and
605 57 DEGs up-regulated). This suggests that tomato plants might repress susceptible factors in
606 order to reduce *B. cinerea* manipulation of host defences (El Oirdi et al., 2011, Temme and
607 Tudzynski, 2009). Interestingly, some of the down-regulated transcripts have cysteine-type
608 peptidase activity (Table S1). These proteins have been reported to have a role in immunity
609 against pathogens including *B.cinerea* (Pogány et al., 2015). Other down-regulated genes are
610 related to plant hormone activity; including ethylene AP2/ERF transcription factors and ABA
611 PYL receptors (SlABAPYL4), reported to be involved in defence responses, which act as
612 positive or negative regulators of JA/ET-dependent defences against *B. cinerea* (Cantu et al.,
613 2009, Moffat et al., 2012). Up-regulated genes included transcripts with peroxidase and
614 transcription regulatory activity, such as peroxidase 5, SlMYB20, SLWRKY51 and
615 SlWRKY72, CONSTANS-like protein with zinc finger binding domain and NAC domain
616 protein and a RING-type E3 ubiquitin transferase involved in protein degradation. These

617 genes have been linked with defence responses (Serrano et al., 2018), which could be result
618 in priming of the tomato immune system against *B. cinerea* infection.
619
620 Transcriptomic (Table S2, Fig S4) and qRT-PCR (Fig S4) analyses showed that chitosan can
621 prime *ACRE75* for a faster and stronger expression after infection with *B. cinerea*. ACRE
622 genes have been linked to plant defence responses. Similar genes were previously identified
623 in tobacco cells to exhibit rapid Cf-9–dependent change in expression through gene-for-gene
624 interaction between the biotroph pathogen *Cladosporium fulvum* avirulence gene (Avr9) and
625 tomato resistance Cf-9 gene (Durrant et al., 2000). To determine the role of ACRE genes in
626 priming by chitosan, we searched for other ACRE genes showing similar expression profiles
627 to *ACRE75* and this revealed that *ACRE180* displays a similar priming profile. This was more
628 evident at 9 hpi (Fig S4) than at 6 hpi, suggesting that the role of ACRE180 is later time than
629 ACRE75. Subcellular localisation may indicate why priming of these genes does not occur at
630 the same time; whereas ACRE75 accumulates exclusively in the nucleus and nucleolus
631 (Figure S6e and f), ACRE180 accrues in the ER and peroxisomes (Figure S6g and h). This
632 suggests different molecular functions of these proteins as they tag different cell organelles.
633 Moreover, it could be plausible that ACRE75 and ACRE180 are part of the same signalling
634 pathway, one working upstream of the other, therefore justifying the delayed transcription
635 and activity of ACRE180.
636
637 The roles of ACRE75 and ACRE180 in chitosan-induced priming were investigated by
638 overexpressing these genes in transient and stable systems, in *N. benthamiana* and
639 Arabidopsis, respectively. Moreover, we aimed to identify any *N. benthamiana* and
640 Arabidopsis ACRE75 and ACRE180 analogues. BLAST analysis of tomato ACRE75
641 identified a very low amino acid identity sequence (39%) and ACRE180 failed to identify

any Arabidopsis homologue. In contrast, *N. benthamiana* ACRE75 and ACRE180 homologues were putatively identified. ACRE75 and ACRE180 lack signal peptides, which suggests they might encode small proteins involved in signalling or antimicrobial activity within the infected cell. Similar to the exclusive production of glucosinolates compounds in Brassica plants (Matthaus & luftmann 2000) it is likely that ACRE75 and ACRE180 are involved in the production of unique compounds to Solanaceae plants. Overexpression of *SlACRE75* and *SlACRE180,* and their *N. benthamiana* orthologues results in induced resistance against *B. cinerea* (Fig 4b and c). Therefore, our results confirm involvement of ACRE genes in plant immunity and suggest an involvement in chitosan-induced priming due to their expression profiles. Interestingly, the induced resistance effect was greater in Arabidopsis plants overexpressing ACRE75 in comparison to ACRE180 (Fig 4c), which could corroborate our evidence of earlier activity of ACRE75, therefore being more effective during early resistance response. More work in needed to unravel the molecular function of ACRE75 and ACRE180 in the expression of priming mechanisms. Nevertheless, fine-tuning of priming-based mechanisms under the control of *SlACRE75*, *SlACRE180*, *NbACRE75* and *NbACRE180* could facilitate its incorporation into other crop species for the enhancement of cross tolerance to old and emergent pest and pathogens, and other challenges. The results unveiled potential molecular pathways involved in chitosan-induced priming of resistance in tomato against *B. cinerea*, potentially applicable to other crops.

Acknowledgement

The authors thank Prof Nicola Stanley-Wall for the academic supervision, Prof Murray Grant for his assistance during HPLC analysis of plant defence hormones, Prof Jurriaan Ton for initial advice on the project, laboratory access, resources, support and intellectual input, Dr Katherine Wright for her

667 support during the confocal microscopy analysis, Dr Colin Alexander for his help with the statistics
668 described in the paper and Dr Mike Roberts for providing spores of *B. cinerea* and extremely valuable
669 input with the microarray analysis. We thank ChiPro GmbH for providing the commercial
670 formulation of chitosan. We are grateful for financial support from the Rural and Environmental
671 Science and Analytical Services (RESAS) Division of the Scottish Government (2011-16) under its
672 Environmental Change and Food, Land and People Research Programmes. This work is funded by
673 AHDB (HDC) Studentship CP105 was secured by A.N and N.H to support D.DV doctoral
674 programme, and the BBSRC Future Leader Fellowship BB/P00556X/1 and BB/P00556X/2 to E.L.

675

676 Author contribution

677 All bioassays were performed by D.DV and E.L. Transcriptome analysis was done by J.M and P.E.H
678 Data analysis was performed by D.DV, N.H, P.E.H and E.L. Intellectual input was provided by
679 D.DV, N.H, P.E.H, E.L and A.N. Project was conceived and supervised by N.H and A.N. The
680 manuscript was written by D.DV and E.L with input from all authors.

681

682 References

683 ARANEGA-BOU, P., DE LA O LEYVA, M., FINITI, I., GARCÍA-AGUSTÍN, P. & GONZÁLEZ-BOSCH, C. 2014.
684 Priming of plant resistance by natural compounds. Hexanoic acid as a model. *Frontiers in*
685 *Plant Science,* 5.
686 CANTU, D., BLANCO-ULATE, B., YANG, L., LABAVITCH, J. M., BENNETT, A. B. & POWELL, A. L. T. 2009.
687 Ripening-Regulated Susceptibility of Tomato Fruit to Botrytis cinerea Requires
688 NOR But Not RIN or Ethylene. *Plant Physiology,* 150**,** 1434-1449.
689 CLOUGH, S. J. & BENT, A. F. 1998. Floral dip: a simplified method for Agrobacterium -mediated
690 transformation of Arabidopsis thaliana. *The Plant Journal,* 16**,** 735-743.
691 CONRATH, U., BECKERS, G. J. M., FLORS, V., GARCÍA-AGUSTÍN, P., JAKAB, G., MAUCH, F., NEWMAN,
692 M.-A., PIETERSE, C. M. J., POINSSOT, B., POZO, M. J., PUGIN, A., SCHAFFRATH, U., TON, J.,
693 WENDEHENNE, D., ZIMMERLI, L. & MAUCH-MANI, B. 2006. Priming: Getting Ready for
694 Battle. *Molecular Plant-Microbe Interactions,* 19**,** 1062-1071.
695 DURRANT, W. E., ROWLAND, O., PIEDRAS, P., HAMMOND-KOSACK, K. E. & JONES, J. D. G. 2000.
696 cDNA-AFLP Reveals a Striking Overlap in Race-Specific Resistance and Wound Response
697 Gene Expression Profiles. *The Plant Cell,* 12**,** 963-977.
698 EL OIRDI, M., EL RAHMAN, T. A., RIGANO, L., EL HADRAMI, A., RODRIGUEZ, M. C., DAAYF, F.,
699 VOJNOV, A. & BOUARAB, K. 2011. Botrytis cinerea manipulates the antagonistic effects
700 between immune pathways to promote disease development in tomato. *The Plant cell,* 23**,**
701 2405-2421.

FARETRA, F. & POLLASTRO, S. 1991. Genetic basis of resistance to benzimidazole and dicarboximide fungicides in Botryotinia fuckeliana (Botrytis cinerea). *Mycological Research,* 95**,** 943-951.

FERNÁNDEZ-CRESPO, E., NAVARRO, J. A., SERRA-SORIANO, M., FINITI, I., GARCÍA-AGUSTÍN, P., PALLÁS, V. & GONZÁLEZ-BOSCH, C. 2017. Hexanoic Acid Treatment Prevents Systemic MNSV Movement in Cucumis melo Plants by Priming Callose Deposition Correlating SA and OPDA Accumulation. *Frontiers in Plant Science,* 8.

FINITI, I., DE LA O. LEYVA, M., VICEDO, B., GÓMEZ-PASTOR, R., LÓPEZ-CRUZ, J., GARCÍA-AGUSTÍN, P., REAL, M. D. & GONZÁLEZ-BOSCH, C. 2014. Hexanoic acid protects tomato plants against Botrytis cinerea by priming defence responses and reducing oxidative stress. *Molecular Plant Pathology,* 15**,** 550-562.

FORCAT, S., BENNETT, M. H., MANSFIELD, J. W. & GRANT, M. R. 2008. A rapid and robust method for simultaneously measuring changes in the phytohormones ABA, JA and SA in plants following biotic and abiotic stress. *Plant Methods,* 4**,** 16.

GAMIR, J., PASTOR, V., KAEVER, A., CEREZO, M. & FLORS, V. 2014. Targeting novel chemical and constitutive primed metabolites against Plectosphaerella cucumerina. *The Plant Journal,* 78**,** 227-240.

GILROY, E. M., TAYLOR, R. M., HEIN, I., BOEVINK, P., SADANANDOM, A. & BIRCH, P. R. J. 2011. CMPG1-dependent cell death follows perception of diverse pathogen elicitors at the host plasma membrane and is suppressed by Phytophthora infestans RXLR effector AVR3a. *New Phytologist,* 190**,** 653-666.

GOY, R. C., BRITTO, D. D. & ASSIS, O. B. G. 2009. A review of the antimicrobial activity of chitosan. *Polímeros,* 19**,** 241-247.

GUAN, Y.-J., HU, J., WANG, X.-J. & SHAO, C.-X. 2009. Seed priming with chitosan improves maize germination and seedling growth in relation to physiological changes under low temperature stress. *Journal of Zhejiang University. Science. B,* 10**,** 427-433.

HAMEED, A., SHEIKH, M. A., FAROOQ, T., BASRA, S. & JAMIL, A. 2013. Chitosan priming enhances the seed germination, antioxidants, hydrolytic enzymes, soluble proteins and sugars in wheat seeds. *Agrochimica,* 57**,** 97-110.

KOHLER, A., SCHWINDLING, S. & CONRATH, U. 2002. Benzothiadiazole-Induced Priming for Potentiated Responses to Pathogen Infection, Wounding, and Infiltration of Water into Leaves Requires the NPR1/NIM1 Gene in Arabidopsis. *Plant Physiology,* 128**,** 1046-1056.

KRÓL, P., IGIELSKI, R., POLLMANN, S. & KĘPCZYŃSKA, E. 2015. Priming of seeds with methyl jasmonate induced resistance to hemi-biotroph Fusarium oxysporum f.sp. lycopersici in tomato via 12-oxo-phytodienoic acid, salicylic acid, and flavonol accumulation. *Journal of Plant Physiology,* 179**,** 122-132.

LA CAMERA, S., L'HARIDON, F., ASTIER, J., ZANDER, M., ABOU-MANSOUR, E., PAGE, G., THUROW, C., WENDEHENNE, D., GATZ, C., MÉTRAUX, J.-P. & LAMOTTE, O. 2011. The glutaredoxin ATGRXS13 is required to facilitate Botrytis cinerea infection of Arabidopsis thaliana plants. *The Plant Journal,* 68**,** 507-519.

LUNA, E. 2016. Using Green Vaccination to Brighten the Agronomic Future. 27**,** 136-140(5).

LUNA, E., BEARDON, E., RAVNSKOV, S., SCHOLES, J. & TON, J. 2016. Optimizing Chemically Induced Resistance in Tomato Against Botrytis cinerea. *Plant Disease,* 100**,** 704-710.

LUNA, E., LÓPEZ, A., KOOIMAN, J. & TON, J. 2014. Role of NPR1 and KYP in long-lasting induced resistance by β-aminobutyric acid. *Frontiers in plant science,* 5**,** 184-184.

LUNA, E., PASTOR, V., ROBERT, J., FLORS, V., MAUCH-MANI, B. & TON, J. 2011. Callose Deposition: A Multifaceted Plant Defense Response. *Molecular Plant-Microbe Interactions,* 24**,** 183-193.

MARTINEZ-MEDINA, A., FLORS, V., HEIL, M., MAUCH-MANI, B., PIETERSE, C. M. J., POZO, M. J., TON, J., VAN DAM, N. M. & CONRATH, U. 2016. Recognizing Plant Defense Priming. *Trends in Plant Science,* 21**,** 818-822.

MAUCH-MANI, B., BACCELLI, I., LUNA, E. & FLORS, V. 2017. Defense Priming: An Adaptive Part of Induced Resistance. *Annual Review of Plant Biology,* 68**,** 485-512.

MCLELLAN, H., BOEVINK, P. C., ARMSTRONG, M. R., PRITCHARD, L., GOMEZ, S., MORALES, J., WHISSON, S. C., BEYNON, J. L. & BIRCH, P. R. J. 2013. An RxLR Effector from Phytophthora infestans Prevents Re-localisation of Two Plant NAC Transcription Factors from the Endoplasmic Reticulum to the Nucleus. *PLOS Pathogens,* 9**,** e1003670.

MOFFAT, C. S., INGLE, R. A., WATHUGALA, D. L., SAUNDERS, N. J., KNIGHT, H. & KNIGHT, M. R. 2012. ERF5 and ERF6 Play Redundant Roles as Positive Regulators of JA/Et-Mediated Defense against Botrytis cinerea in Arabidopsis. *PLOS ONE,* 7**,** e35995.

MUÑOZ, Z. & MORET, A. 2010. Sensitivity of Botrytis cinerea to chitosan and acibenzolar-S-methyl. *Pest Management Science,* 66**,** 974-979.

OERKE, E. C. 2006. Crop losses to pests. *The Journal of Agricultural Science,* 144**,** 31-43.

OIDE, S., BEJAI, S., STAAL, J., GUAN, N., KALIFF, M. & DIXELIUS, C. 2013. A novel role of PR2 in abscisic acid (ABA) mediated, pathogen-induced callose deposition in Arabidopsis thaliana. *New Phytologist,* 200**,** 1187-1199.

PAPPAS, A. C. 1997. Evolution of fungicide resistance in Botrytis cinerea in protected crops in Greece. *Crop Protection,* 16**,** 257-263.

POGÁNY, M., DANKÓ, T., KÁMÁN-TÓTH, E., SCHWARCZINGER, I. & BOZSÓ, Z. 2015. Regulatory Proteolysis in Arabidopsis-Pathogen Interactions. *International journal of molecular sciences,* 16**,** 23177-23194.

POZO, M. J., LÓPEZ-RÁEZ, J. A., AZCÓN-AGUILAR, C. & GARCÍA-GARRIDO, J. M. 2015. Phytohormones as integrators of environmental signals in the regulation of mycorrhizal symbioses. *New Phytologist,* 205**,** 1431-1436.

QIN, P., FAN, S., DENG, L., ZHONG, G., ZHANG, S., LI, M., CHEN, W., WANG, G., TU, B., WANG, Y., CHEN, X., MA, B. & LI, S. 2018. LML1, Encoding a Conserved Eukaryotic Release Factor 1 Protein, Regulates Cell Death and Pathogen Resistance by Forming a Conserved Complex with SPL33 in Rice. *Plant and Cell Physiology,* 59**,** 887-902.

RAAFAT, D. & SAHL, H.-G. 2009. Chitosan and its antimicrobial potential--a critical literature survey. *Microbial biotechnology,* 2**,** 186-201.

RAMÍREZ-CARRASCO, G., MARTÍNEZ-AGUILAR, K. & ALVAREZ-VENEGAS, R. 2017. Transgenerational Defense Priming for Crop Protection against Plant Pathogens: A Hypothesis. *Frontiers in Plant Science,* 8**,** 696.

REDMAN, A., CIPOLLINI, D. & SCHULTZ, J. 2001. Fitness costs of jasmonic acid-induced defense in tomato, Lycopersicon esculentum. *Oecologia,* 126**,** 380-385.

REECE-HOYES, J. S. & WALHOUT, A. J. M. 2018. Gateway Recombinational Cloning. *Cold Spring Harbor protocols,* 2018**,** pdb.top094912-pdb.top094912.

REJEB, I. B., PASTOR, V., GRAVEL, V. & MAUCH-MANI, B. 2018. Impact of β-aminobutyric acid on induced resistance in tomato plants exposed to a combination of abiotic and biotic stress. *Journal of Agricultural Science and Botany,* 2.

ROBERT-SEILANIANTZ, A., GRANT, M. & JONES, J. D. G. 2011. Hormone Crosstalk in Plant Disease and Defense: More Than Just JASMONATE-SALICYLATE Antagonism. *Annual Review of Phytopathology,* 49**,** 317-343.

ROMANAZZI, G., FELIZIANI, E., SANTINI, M. & LANDI, L. 2013. Effectiveness of postharvest treatment with chitosan and other resistance inducers in the control of storage decay of strawberry. *Postharvest Biology and Technology,* 75**,** 24-27.

SATHIYABAMA, M., AKILA, G. & EINSTEIN CHARLES, R. 2014. Chitosan-induced defence responses in tomato plants against early blight disease caused by Alternaria solani (Ellis and Martin) Sorauer. *Archives of Phytopathology and Plant Protection,* 47**,** 1777-1787.

SAVARY, S., FICKE, A., AUBERTOT, J. N. & HOLLIER, C. 2012. Crop losses due to diseases and their implications for global food production losses and food security. *Food Security,* 4**,** 519-537.

SCALSCHI, L., SANMARTÍN, M., CAMAÑES, G., TRONCHO, P., SÁNCHEZ-SERRANO, J. J., GARCÍA-AGUSTÍN, P. & VICEDO, B. 2015. Silencing of OPR3 in tomato reveals the role of OPDA in callose deposition during the activation of defense responses against Botrytis cinerea. *The Plant Journal,* 81**,** 304-315.

SERRANO, I., CAMPOS, L. & RIVAS, S. 2018. Roles of E3 Ubiquitin-Ligases in Nuclear Protein Homeostasis during Plant Stress Responses. *Frontiers in plant science,* 9**,** 139-139.

SLAUGHTER, A., DANIEL, X., FLORS, V., LUNA, E., HOHN, B. & MAUCH-MANI, B. 2012. Descendants of Primed Arabidopsis Plants Exhibit Resistance to Biotic Stress. *Plant Physiology,* 158**,** 835-843.

TEMME, N. & TUDZYNSKI, P. 2009. Does Botrytis cinerea Ignore H 2 O 2 -Induced Oxidative Stress During Infection? Characterization of Botrytis Activator Protein 1. *Molecular plant-microbe interactions : MPMI,* 22**,** 987-98.

THOMAS, P. D., CAMPBELL, M. J., KEJARIWAL, A., MI, H., KARLAK, B., DAVERMAN, R., DIEMER, K., MURUGANUJAN, A. & NARECHANIA, A. 2003. PANTHER: A Library of Protein Families and Subfamilies Indexed by Function. *Genome Research,* 13**,** 2129-2141.

TON, J., JAKAB, G., TOQUIN, V., FLORS, V., IAVICOLI, A., MAEDER, M. N., MÉTRAUX, J.-P. & MAUCH-MANI, B. 2005. Dissecting the β-Aminobutyric Acid–Induced Priming Phenomenon in Arabidopsis. *The Plant Cell,* 17**,** 987-999.

VAN DEN BURG, H. A., TSITSIGIANNIS, D. I., ROWLAND, O., LO, J., RALLAPALLI, G., MACLEAN, D., TAKKEN, F. L. W. & JONES, J. D. G. 2008. The F-box protein ACRE189/ACIF1 regulates cell death and defense responses activated during pathogen recognition in tobacco and tomato. *The Plant cell,* 20**,** 697-719.

VAN HULTEN, M., PELSER, M., VAN LOON, L. C., PIETERSE, C. M. J. & TON, J. 2006. Costs and benefits of priming for defense in Arabidopsis. *Proceedings of the National Academy of Sciences,* 103**,** 5602-5607.

VASSEUR, F., BRESSON, J., WANG, G., SCHWAB, R. & WEIGEL, D. 2018. Image-based methods for phenotyping growth dynamics and fitness components in Arabidopsis thaliana. *Plant Methods* [Online], 14. [Accessed 2018].

WANG, K., LIAO, Y., KAN, J., HAN, L. & ZHENG, Y. 2014. Response of direct or priming defense against Botrytis cinerea to methyl jasmonate treatment at different concentrations in grape berries. *International journal of food microbiology,* 194C**,** 32-39.

WARD, N. & MORENO-HAGELSIEB, G. 2014. Quickly Finding Orthologs as Reciprocal Best Hits with BLAT, LAST, and UBLAST: How Much Do We Miss? *PLOS ONE,* 9**,** e101850.

WILKINSON, S. W., PASTOR, V., PAPLAUSKAS, S., PÉTRIACQ, P. & LUNA, E. 2018. Long-lasting β-aminobutyric acid-induced resistance protects tomato fruit against Botrytis cinerea. *Plant Pathology,* 67**,** 30-41.

WILLIAMSON, B., TUDZYNSKI, B., TUDZYNSKI, P. & VAN KAN, J. A. L. 2007. Botrytis cinerea: the cause of grey mould disease. *Molecular Plant Pathology,* 8**,** 561-580.

WORRALL, D., HOLROYD, G. H., MOORE, J. P., GLOWACZ, M., CROFT, P., TAYLOR, J. E., PAUL, N. D. & ROBERTS, M. R. 2012. Treating seeds with activators of plant defence generates long-lasting priming of resistance to pests and pathogens. *New Phytologist,* 193**,** 770-778.

YANG, L., MCLELLAN, H., NAQVI, S., HE, Q., BOEVINK, P. C., ARMSTRONG, M., GIULIANI, L. M., ZHANG, W., TIAN, Z., ZHAN, J., GILROY, E. M. & BIRCH, P. R. J. 2016. Potato NPH3/RPT2-Like Protein StNRL1, Targeted by a Phytophthora infestans RXLR Effector, Is a Susceptibility Factor. *Plant Physiology,* 171**,** 645-657.

YOUNES, I., HAJJI, S., FRACHET, V., RINAUDO, M., JELLOULI, K. & NASRI, M. 2014. Chitin extraction from shrimp shell using enzymatic treatment. Antitumor, antioxidant and antimicrobial activities of chitosan. *International Journal of Biological Macromolecules,* 69**,** 489-498.

ZIMMERLI, L., JAKAB, G., MÉTRAUX, J.-P. & MAUCH-MANI, B. 2000. Potentiation of pathogen-specific defense mechanisms in Arabidopsis by β-aminobutyric acid. *Proceedings of the National Academy of Sciences,* 97**,** 12920-12925.

Tables

Table 1: Biological processes and molecular functions of enriched genes

GO biological processes for Chitosan + B.cinerea at 6 hpi						
	S. lycopersicum ref. #	Upload #	Expected	Fold Enrichmer	+/-	P value <0.05
response to auxin	209	10	1.58	6.35	+	9.47E-03
response to chemical	916	20	6.91	2.9	+	4.55E-02
response to stimulus	2657	44	20.03	2.2	+	1.25E-03
Unclassified	17617	117	132.83	0.88	-	0.00E+00

GO molecular functions for Chitosan + B.cinerea at 6 hpi						
	S. lycopersicum ref. #	Upload #	Expected	Fold Enrichmer	+/-	P value <0.05
cysteine-type peptidase activity	271	11	2.04	5.38	+	1.23E-02
transcription factor activity, sequence-specific DNA binding	856	19	6.45	2.94	+	4.78E-02
nucleic acid binding transcription factor activity	856	19	6.45	2.94	+	4.78E-02
Unclassified	16331	109	123.14	0.89	-	0.00E+00

To include in page 19 line 449

Figure Legends

Figure 1. Characterisation of chitosan-induced resistance in tomato and Arabidopsis. (a) Disease lesions in tomato and (b) in Arabidopsis at 3 days post inoculation. Values represent means ± SEM (n=4-10). (c) Callose deposition triggered by chitosan treatment in tomato and (d) in Arabidopsis 1 day post treatment. Values represent means ± SEM (n=8-10) of % of callose per leaf area. Different letters indicate statistically significant differences among treatments (Least Significant Differences for graph a and Dunnett T3 Post-Hoc test for graphs b, c and d, α=0.05).

Figure 2. Chitosan-induced resistance is based on priming. **(a)** Disease lesions in tomato at 3 days post inoculation (dpi) 2 weeks after treatment with water (Control) or 1% chitosan.

Values represent means ± SEM (n=8). Asterisk indicates statistically significant differences among treatments (Student's T. test, α=0.05). **(b)** Percentage of callose deposited at the infection site in water (Control) and chitosan (0.01%)-treated plants compared to the fungal lesion diameter at 1 day after infection with *B. cinerea*. Values represent means ± SEM (n=4). Asterisk indicates statistically significant differences among treatments (Student's T. test, α=0.05). **(c)** Representative pictures of chitosan-induced priming of callose at the infection site. Blue colours correspond to fungal growth whereas yellow colours correspond with the callose deposition at the infection site. Scale bars= 0.5 mm. **(d)** Mass-spectrometry quantification (ng/mL) of Salicylic acid (SA), Jasmonic acid (JA) and Abscisic acid (ABA) at 24h post infection. Values represent means ± SEM (n=4). letters indicates statistically significant differences among treatments (Least Significant Differences, α=0.05, n.s. = not significant).

Figure 3. Transcriptome analysis of chitosan-induced resistance against *Botrytis cinerea*. **(a)** Principal component analysis (PCA) of whole transcriptional microarray at 6, 9 and 12 hour post infection (hpi). **(b)** Heatmap of differentially expressed genes (2-way ANOVA $p < 0.01$, Bonferoni), clustered by expression. Profiles are shown +/- treatment with chitosan and infection with *B. cinerea* at 6, 9, 12 hpi logarithmic scale fold induced (red) or repressed (blue) compared to Water + Mock. Hierarchical clusters on expression profile are broadly classed as i, ii, iii or iv. **(c)** Venn diagram of statistically significant data set (2-way ANOVA $p < 0.01$, Benjamin–Hochberg) of differentially expressed genes. Pairwise Student's T-test comparisons were performed (Volcano plots: $p < 0.05$, 2-fold cut-off) for the three test treatments (Chitosan + Mock, Water + *B. cinerea* and Chitosan + *B. cinerea*) compared to control treatment (Water + Mock) at 6, 9 and 12 hpi.

Figure 4. Functional characterisation of ACRE genes. **(a)** Chitosan-induced resistance in *Nicotiana benthamiana*. Disease lesions at 2 days post inoculation (dpi). Values represent means ± SEM (n=18). Asterisk indicates statistically significant differences between treatments (Student's T. test, α=0.05). **(b)** Transient expression of constitutively active SlACRE75, SlACRE180, NbACRE75 and NbACRE180 in *N. benthamiana* against *B. cinerea*. Lesion size measurements were performed at 4 days post-infection (dpi). Values presented are means ± SEM (n=6). Different letters indicate statistically significant differences (ANOVA $p < 0.05$ followed by Tukey's Post-hoc at 4 dpi). **(c)** *A. thaliana* transformed overexpression stable SlACRE75, SlACRE180, NbACRE75 and NbACRE180 infected with *B. cinerea*. Lesion sizes were measured at 6 days after inoculation (dpi). Values presented are means ± SEM (n=8-16). Asterisks indicate statistically significant differences (* $p < 0.05$, ** $p < 0.01$; *** $p < 0.001$).

Figure S1. Chitosan-induced resistance in *Solanaceae melongena* (aubergine). Disease lesions at 3 dpi. Values represent means ± SEM (n=10). Different letters indicate statistically significant differences among treatments (Least Significant Differences, α=0.05).

Figure S2. Chitosan and Switch fungicide antifungal activity against *Botrytis cinerea*. Bars represent means of fungal growth diameter (± SEM, n=5) at 4 days after inoculating PDA-containing Petri dishes with 5 mm agar plugs of actively growing *B. cinerea* mycelia. Different letters indicate statistically significant differences among treatments (Least Significant Differences, α=0.05)

948 **Figure S3. Chitosan-induced resistance is based on priming**. **(a)** Relative Growth Rate
949 (RGR) per week of tomato plants 1 and 2 weeks after treatment with 0.01% chitosan. Values
950 represent means ± SEM (n=10). Asterisk indicates statistically significant differences among
951 treatments (Student's T. test, α=0.05) **(b)** Mass-spectrometry quantification (% of peak area)
952 of Jasmonic acid-isoleucine (JA-ile) at 24h post inoculation. Values represent means ± SEM
953 (n=4). Different letters indicate statistically significant differences among treatments (Least
954 Significant Differences, α=0.05)

955

956 **Figure S4. Validation of microarray expression results**. Expression profile obtained in the
957 microarray (a) and in the analysis by RT-q-PCR (b) of a subset of 9 genes at 9 hpi with
958 *Botrytis cinerea*

959

960 **Figure S5. Western Blot analysis**. Expression of proteins by immunoblot analysis of GFP-
961 SlACRE75, GFP-SlACRE180, GFP-NbACRE75 and GFP-NbACRE180 fusion proteins in
962 *N. benthamiana* leaves at 48 h after agroinfiltration. Expected protein sizes were (i)
963 SlACRE75= 14.79 + 26 KDa GFP= 40.8 KDa; (ii) SlACRE180= 10.86 +26= 36.8 KDa; (iii)
964 NbACRE180= 11.74+26= 37.7 KDa; and (iv) NbACRE75= 14.6+26= 40.7 Kda. Proteins
965 were separated by SDS–PAGE and analysed by immunoblotting. A GFP-specific antibody
966 was used for detection of GFP-fusion protein. Equal loading of total proteins was examined
967 by Ponceau staining (PS). Three lanes represent 3 replicates per construct GFP-SlACRE75,
968 GFP-SlACRE180, GFP-NbACRE75, GFP-NbACRE180, and a GFP-non-protein/ empty
969 vector (control).

970

Figure S6. Subcellular location of ACRE proteins. Confocal microscopy observation of **(a)** pFlub vector as a RFP-peroxisome tagged marker, **(b)** nucleus mRFP marker, **(c)** ER mRFP marker, **(d)** free GFP in cytoplasm and the nucleus, **(e)** GFP-SlACRE75 and **(f)** GFP-NbACRE75 fusions in the nucleus and nucleolus, **(g)** GFP-SlACRE180 fusion in the ER and **(h)** GFP-NbACRE180 fusion in the peroxisomes.

Figure S7. Growth analysis. Perimeter in cm of rosettes from Arabidopsis lines overexpressing GFP-Empty vector (EV), GFP-SlACRE75, GFP-SlACRE180, GFP-NbACRE75 and GFP-NbACRE180 constructs. Values represent means ± SEM (n=8-16). n.s = not significant differences between treatments (One-way ANOVA, α=0.05)

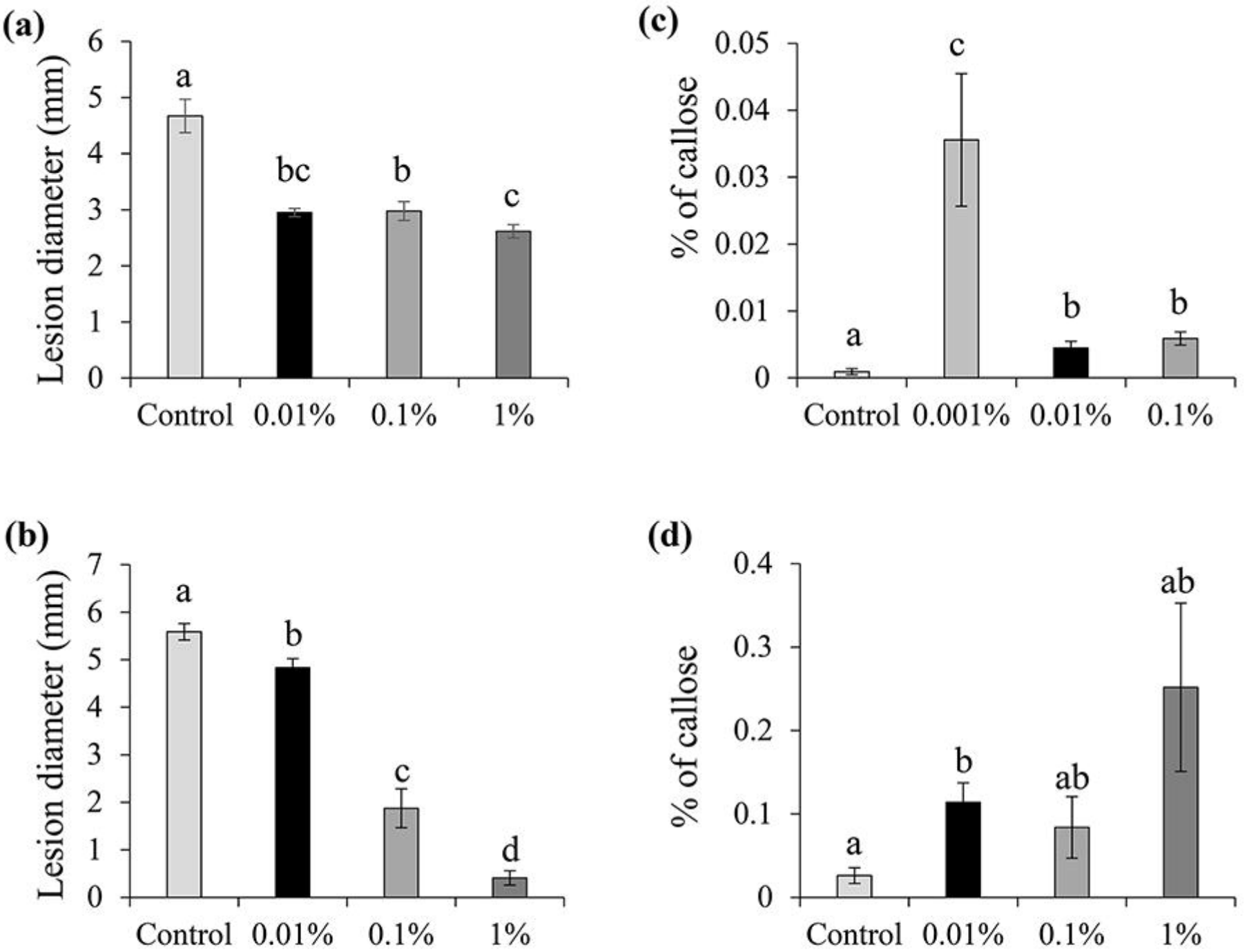
(a)
Lesion diameter (mm)
0
1
2
3
4
5
6
a
bc
b
c
Control
0.01%
0.1%
1%
(c)
% of callose
0
0.01
0.02
0.03
0.04
0.05
a
c
b
b
Control
0.001%
0.01%
0.1%
(b)
Lesion diameter (mm)
0
1
2
3
4
5
6
7
a
b
c
d
Control
0.01%
0.1%
1%
(d)
% of callose
0
0.1
0.2
0.3
0.4
a
b
ab
ab
Control
0.01%
0.1%
1%

Figure 1

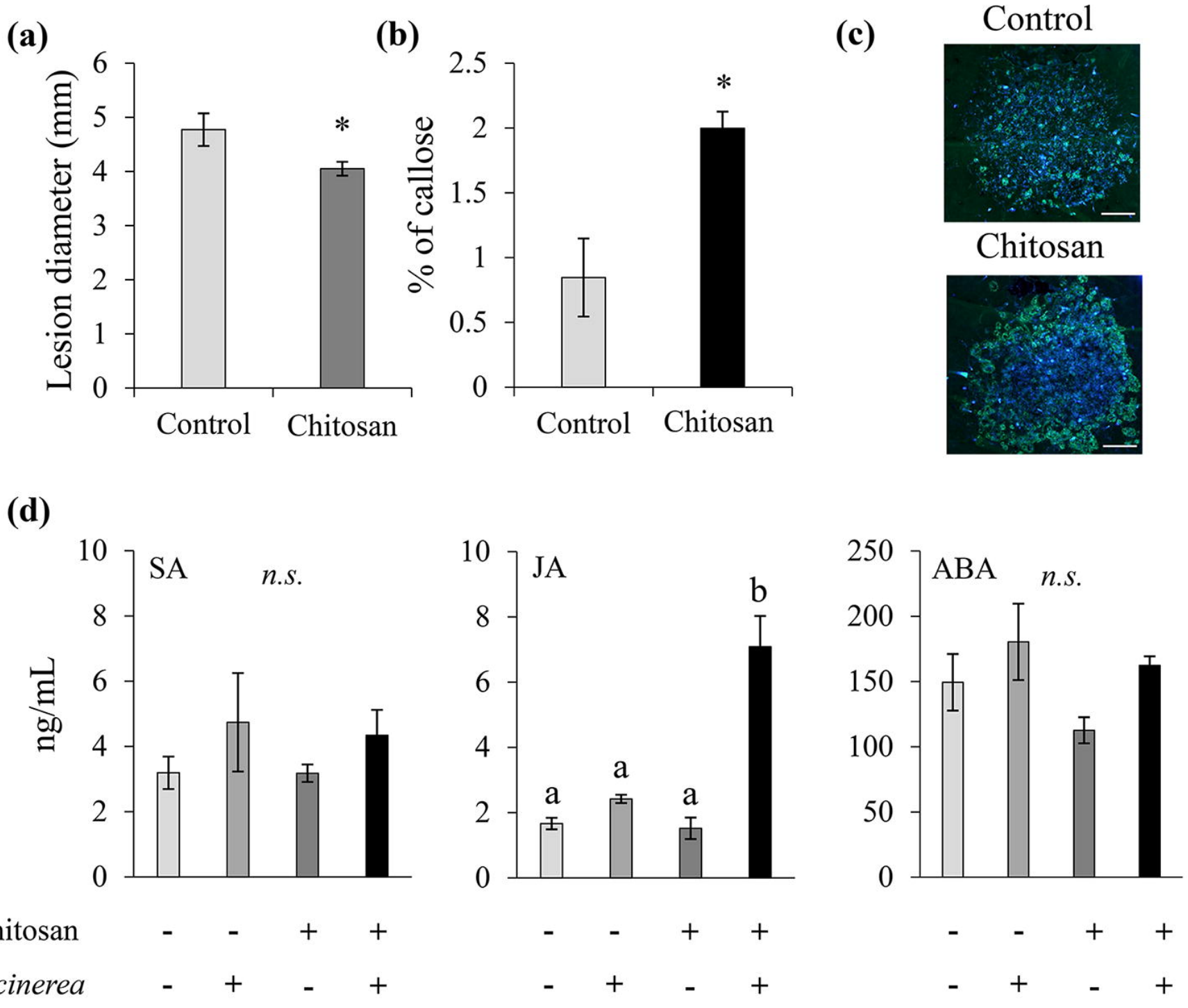
(a)
Lesion diameter (mm)
6
5
4
3
2
1
0
*
Control
Chitosan
(b)
% of callose
2.5
2
1.5
1
0.5
0
*
Control
Chitosan
(c)
Control
Chitosan
(d)
ng/mL
10
8
6
4
2
0
SA
n.s.
JA
a
a
a
b
250
200
150
100
50
ABA
n.s.
Chitosan
B. cinerea
- - + +
- + - +

Figure 2

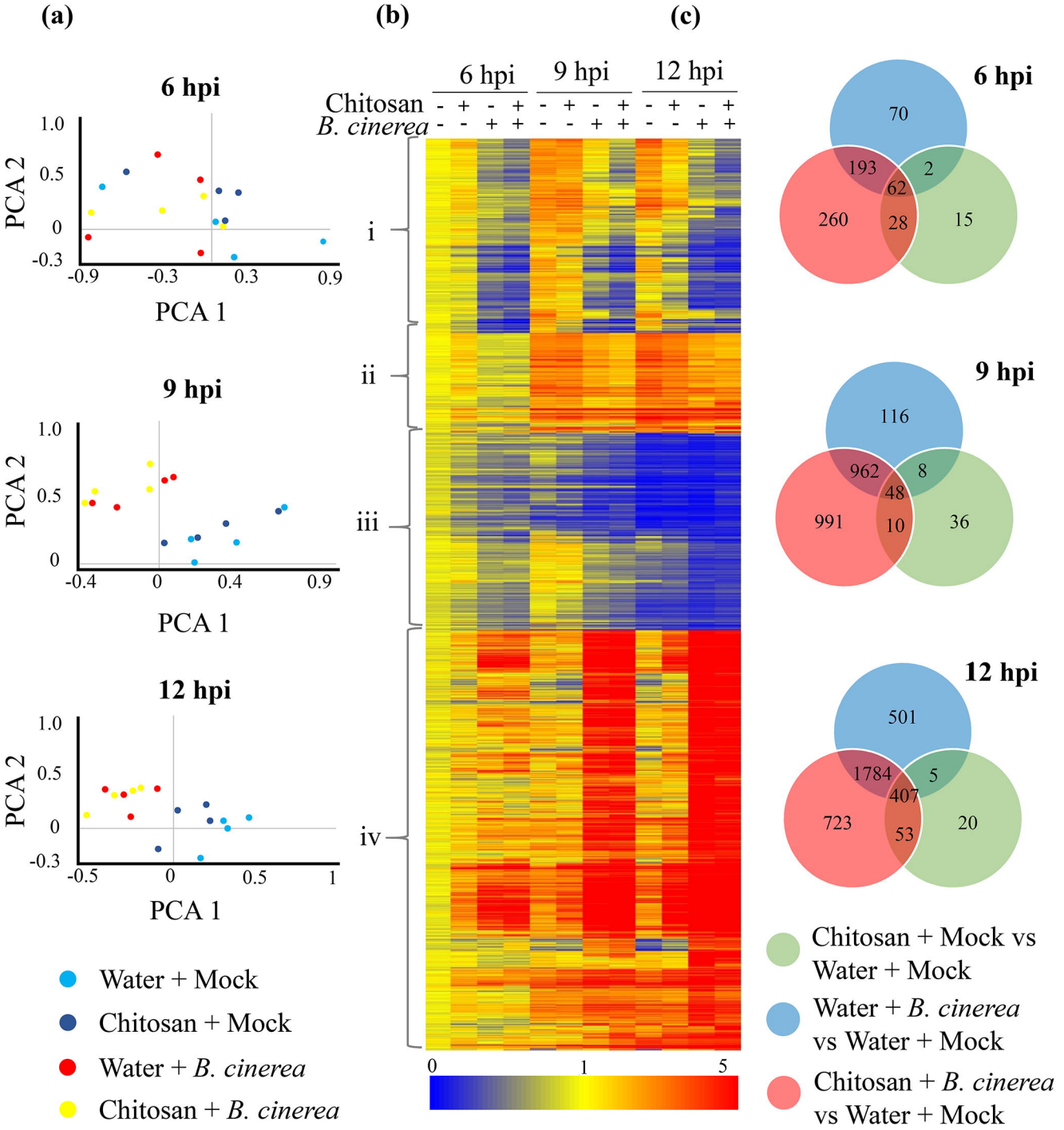
(a)
6 hpi
PCA 2
PCA 1
9 hpi
12 hpi
Water + Mock
Chitosan + Mock
Water + B. cinerea
Chitosan + B. cinerea
(b)
6 hpi
9 hpi
12 hpi
Chitosan
B. cinerea
i
ii
iii
iv
(c)
6 hpi
70
193
2
62
260
28
15
9 hpi
116
962
8
48
991
10
36
12 hpi
501
1784
5
407
723
53
20
Chitosan + Mock vs Water + Mock
Water + B. cinerea vs Water + Mock
Chitosan + B. cinerea vs Water + Mock

Figure 3

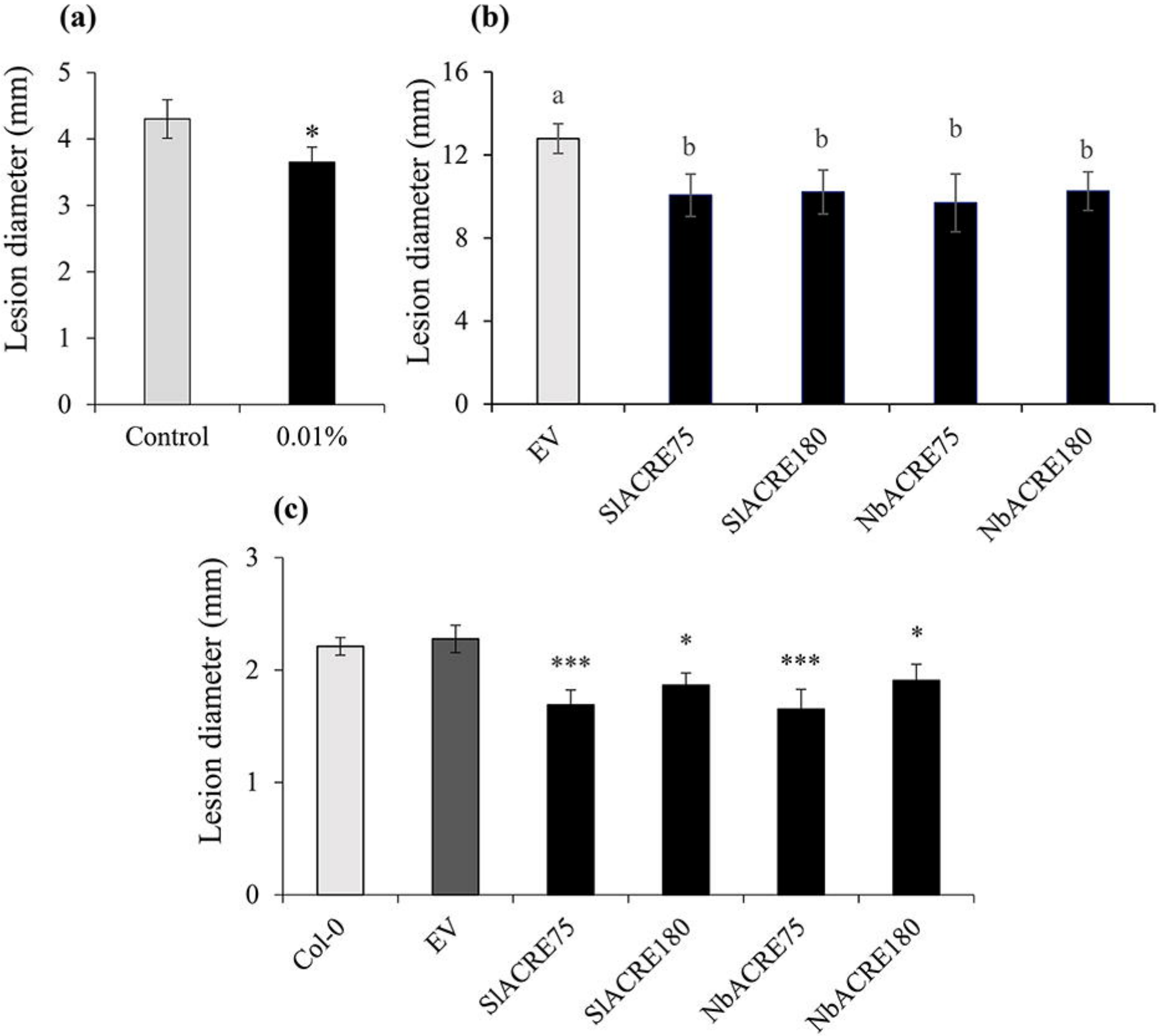
(a)
Lesion diameter (mm)
5
4
3
2
1
0
*
Control
0.01%
(b)
Lesion diameter (mm)
16
12
8
4
0
a
b
b
b
b
EV
SlACRE75
SlACRE180
NbACRE75
NbACRE180
(c)
Lesion diameter (mm)
3
2
1
0
***
*
***
*
Col-0
EV
SlACRE75
SlACRE180
NbACRE75
NbACRE180

Figure 4